Revisiting the Concepts of Return Period and Risk for Nonstationary Hydrologic Extreme Events

Jose D. Salas, M.ASCE[1]; and Jayantha Obeysekera, M.ASCE[2]

Abstract: Current practice using probabilistic methods applied for designing hydraulic structures generally assume that extreme events are stationary. However, many studies in the past decades have shown that hydrological records exhibit some type of nonstationarity such as trends and shifts. Human intervention in river basins (e.g., urbanization), the effect of low-frequency climatic variability (e.g., Pacific Decadal Oscillation), and climate change due to increased greenhouse gasses in the atmosphere have been suggested to be the leading causes of changes in the hydrologic cycle of river basins in addition to changes in the magnitude and frequency of extreme floods and extreme sea levels. To tackle nonstationarity in hydrologic extremes, several approaches have been proposed in the literature such as frequency analysis, in which the parameters of a given model vary in accordance with time. The aim of this paper is to show that some basic concepts and methods used in designing flood-related hydraulic structures assuming a stationary world can be extended into a nonstationary framework. In particular, the concepts of return period and risk are formulated by extending the geometric distribution to allow for changing exceeding probabilities over time. Building on previous developments suggested in the statistical and climate change literature, the writers present a simple and unified framework to estimate the return period and risk for nonstationary hydrologic events along with examples and applications so that it can be accessible to a broad audience in the field. The applications demonstrate that the return period and risk estimates for nonstationary situations can be quite different than those corresponding to stationary conditions. They also suggest that the nonstationary analysis can be helpful in making an appropriate assessment of the risk of a hydraulic structure during the planned project-life. **DOI: 10.1061/(ASCE)HE.1943-5584.0000820.**

Author keywords: Nonstationarity; Risk; Return period; Extreme floods; Extreme sea levels; Uncertainty.

Introduction

Statistical methods are routinely applied for analyzing a number of problems in hydrology and water resources. This is because most, if not all, hydrological processes such as extreme events have some degree of randomness. The majority of the literature on probabilistic methods applied for designing hydraulic structures assumes that extreme hydrologic events are stationary. However, research has documented that in some places hydrological records exhibit some type of nonstationarity in the form of increasing or decreasing trends (e.g., Olsen et al. 1999; Strupzewski et al. 2001; Douglas et al. 2000; Lins and Slack 1999), upward or downward shifts (e.g., Potter 1976; Salas and Boes 1980; McCabe and Wolock 2002; Franks and Kuczera 2002; Sveinsson et al. 2003; Kiem et al. 2003; Fortin et al. 2004; Akintug and Rasmussen 2005), or a combination of them (Villarini et al. 2009a). Human intervention is one of the leading causes of changes in the hydrologic cycle of river basins. For example, precipitation and streamflow records may be changing due to the effect of land-use changes in basins, such as increasing urbanization (e.g., Konrad and Booth 2002; Villarini et al. 2009b; Hejazi and Markus 2009; Vogel et al. 2011), agricultural developments (e.g., Schilling and Libra 2003; Pielke et al. 2007), and large-scale deforestation (e.g., Gash and Nobre 1997). These intrusions in the landscape change hydrologic response characteristics such as the magnitude and timing of extreme floods.

In addition, it has become apparent that some of the changes that researchers may be observing in hydrological records may be due to the effect of natural climatic variability, particularly resulting from low-frequency components of climate variability such as the El Niño Southern Oscillation (ENSO) and decadal and multidecadal oscillations such as the Pacific Decadal Oscillation (PDO) and Atlantic Multidecadal Oscillation (AMO). These large-scale forcings exert in-phase and out-of-phase oscillations in the magnitude of hydrologic events such as extreme precipitation, extreme floods, droughts, and extreme sea levels (e.g., Mantua et al. 1997; Jain and Lall 2000, 2001; Enfield et al. 2001; McCabe and Wolock 2002; Franks and Kuczera 2002; Keim et al. 2003; Park et al. 2010, 2011).

Another reason for increased attention to nonstationarity is the growing concern on climate change due to increased greenhouse gases in the atmosphere (IPCC 2007). As a consequence the Earth's climate may be changing and in turn causing changes to extreme precipitation, temperature, and floods in certain parts of the globe. Whereas the significance of impacts on some aspects of the hydrological cycle such as streamflows remains debatable and inconclusive (e.g., Cohn and Lins 2005; Hirsch and Ryberg 2012), some hydrologists have declared that "stationarity is dead" (Milly et al. 2008), and suggest that nonstationary probabilistic models need to be identified and possibly used in some practical cases. Furthermore, warming associated with climate change may be causing sea-level rising globally and recent projections of sea level include varying degrees of acceleration in the sea-level rise rate

[1]Professor Emeritus, Dept. of Civil and Environmental Engineering, Colorado State Univ., Fort Collins, CO 80523 (corresponding author). E-mail: jsalas@engr.colostate.edu

[2]Chief Modeler, Hydrologic and Environmental Systems Modeling, South Florida Water Management District, 3301 Gun Club Rd., West Palm Beach, FL 33406. E-mail: jobey@sfwmd.gov

Note. This manuscript was submitted on October 3, 2012; approved on March 26, 2013; published online on April 1, 2013. Discussion period open until August 1, 2014; separate discussions must be submitted for individual papers. This paper is part of the ***Journal of Hydrologic Engineering***, Vol. 19, No. 3, March 1, 2014. © ASCE, ISSN 1084-0699/2014/3-554-568/$25.00.

(e.g., Bindoff et al. 2007; Rahmstorf 2007; Vermeer and Rahmstorf 2009; Obeysekera et al. 2012; Sallenger et al. 2012). Such increases in sea levels are expected to increase flooding due to storm surges in coastal regions and reduce the reliability of flood-protection systems in coastal watersheds (Obeysekera et al. 2011). Furthermore, climate change research suggests that the intensity and rainfall associated with major tropical storms may also increase (Kunkel et al. 2010), potentially leading to increased rainfall-induced flooding in areas exposed to such storms, although the tropical storm frequency globally may decrease in the future (Knutson et al. 2010).

To tackle nonstationarity of hydrologic extremes, several approaches have been proposed in the literature such as frequency-analysis methods, in which the parameters (or moments such as the mean and variance) of a given distribution (e.g., the Gumbel) may vary in accordance with time. They include the following: (1) probability distribution models imbedded with trend components (e.g., Strupczewski et al. 2001; El Adlouni et al. 2007; Cooley 2013; Katz 2013), (2) stochastic models considering shifting patterns (e.g., Sveinsson et al. 2005), (3) models considering covariates (e.g., Katz et al. 2002; Griffis and Stedinger 2007; Villarini et al. 2009b, 2010), and (4) probability distributions with mixed components (e.g., Waylen and Caviedes 1986; Rossi et al. 1984). Multicentury climatic fluctuations have been incorporated into paleoflood frequency-analysis techniques and the analysis of wet and dry periods (e.g., Stedinger and Cohn 1986; Frances et al. 1994; Biondi et al. 2008). In addition, some pragmatic approaches to deal with nonstationarity in flood-frequency analysis have been suggested, such as adjusting the nonstationary peak discharges and applying hydrologic models [taking into account the spatially and temporally varying land-use (Moglen 2003), and adjusting flood records for the combined effects of urbanization and climatic change (Gilroy and McCuen 2012)]. Likewise, a flood-frequency analysis framework that involves a process-based derived flood frequency and risk estimation considering possible future evolution of climatic states has been proposed (Sivapalan and Samuel 2009). Furthermore, similar nonstationary approaches have been proposed for analyzing extreme sea levels (e.g., Caires et al. 2006; Menendez and Woodworth 2010; Ruggiero et al. 2010; Park et al. 2011; Obeysekera et al. 2012).

The aim of this paper is to show that some basic concepts and methods used in designing flood-related hydraulic structures (e.g., flood walls and drainage systems) assuming a stationary world can be extended into a nonstationary framework. In particular, the concepts of return period and risk are formulated by extending the geometric distribution to allow for changing exceedance probabilities over time. As will be documented in the next section, some of these concepts have been previously suggested, particularly in the statistical and climate change journals. However, perhaps because of the complex notation and derivations involved, it appears that insufficient attention has been given in the water-resources engineering literature. Therefore, the main objective of this paper is to present a simple and unified framework along with examples and applications so that it can be accessible to a broader audience in the field.

Brief Review of Existing Concepts and Methods

The traditional methods for determining the return period and risk of extreme hydrologic events assume two key conditions, as follows: (1) extreme events arise from a stationary distribution, and (2) the occurrences of extreme events are independent or weakly dependent (Leadbetter 1983.) The existing methods are reviewed in this section as background information considering the case

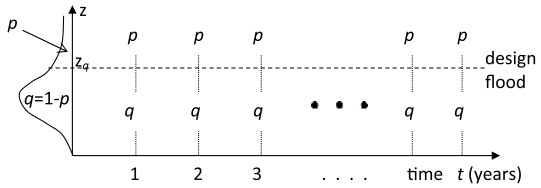

Fig. 1. Schematic depicting the design flood z_q in addition to constant values of exceeding (p) and nonexceeding ($q = 1 - p$) probabilities throughout years 1 to t, i.e., stationary condition

of extreme annual floods. The writers will assume that the annual floods denoted by the random variable Z have a cumulative distribution function (CDF) denoted by $F_Z(z, \underline{\theta})$, where $\underline{\theta}$ is the parameter set. The writers assume that a flood-related hydraulic structure, such as a flood wall, has been designed based on the existing flood record and that the design flood is denoted as z_T, where T (years) is the return period of such a design flood. For convenience, the writers will also use the notation z_q, which is the design flood quantile with nonexceedance probability q, or the flood with exceedance probability $p = 1 - q$. Fig. 1 shows schematically the design flood z_q and that each year the probability of exceeding the design flood is $p = 1 - q$. This means that each year the risk that a flood may exceed z_q remains the same, i.e., the stationary condition.

Thus, assuming independence and stationarity it may be shown that the return period is related to p and q as $T = 1/p = 1/(1 - q)$ (e.g., Gumbel 1941). Examining the fundamental concepts behind this definition will be useful for understanding those for nonstationary conditions. In the mentioned flood design problem the value of T is commonly selected from design manuals and the corresponding design flood z_q is determined from frequency analysis of the underlying flood data, i.e., from the fitted distribution $F_Z(z, \underline{\theta})$.

Researchers would like to answer the question of the probability that a flood exceeding the design flood will occur for the first time in year x. That first time could be in year 1, 2, 3, or so on, or perhaps it will never occur. The waiting time for an exceeding flood to occur for the first time is a random variable that the writers will denote by X. Thus, for a flood (that exceeds the design flood z_q) to occur for the first time in year $X = x$ the following event must occur:

$$\text{Year} \quad 1 \quad 2 \quad 3 \quad \ldots \quad x-1 \quad x \tag{1a}$$

$$\text{Event} \quad \text{NF} \quad \text{NF} \quad \text{NF} \quad \ldots \quad \text{NF} \quad \text{F} \tag{1b}$$

$$\text{Probability} \quad 1-p \quad 1-p \quad 1-p \quad \ldots \quad 1-p \quad p \tag{1c}$$

in which NF = no flood event that exceeds the design flood z_q; and F = flood event that exceeds the design flood z_q. Hence, considering that the yearly floods are independent, the referred event has probability $(1 - p)^{x-1} p$ or

$$f(x) = P(X = x) = (1 - p)^{x-1} p, \; x = 1, 2, \ldots \tag{2}$$

which is the geometric probability law (Mood et al. 1974). $\mathrm{E}(X) = 1/p$, i.e., the mean expected time (or the mean number of years that will take for the first occurrence of a flood exceeding the design flood) is $1/p$, and that is known as the return period T in engineering practice (e.g., Chow et al. 1988). Furthermore, the variance $\mathrm{var}(X) = q/p^2$.

With the foregoing background the writers can now define hydrologic risk. The failure of the hydraulic structure designed for a project life of n years will occur whenever the first arrival

J. Hydrol. Eng. 2014.19:554-568.

of a flood exceeding the design flood occurs before or at year n, i.e., $R = P(X \le n) = F_X(n)$, where $F_X(x)$ is the CDF of the geometric distribution

$$R = \sum_{x=1}^{n} f(x) = p \sum_{x=1}^{n} (1-p)^{x-1} = 1 - (1-p)^n \qquad (3)$$

The reliability R_ℓ of the structure is then $1 - R$ or

$$R_\ell = (1-p)^n \qquad (4)$$

The reliability is the probability P that no floods exceeding the design flood z_q will occur in the n-year period, i.e., $P(Y = 0)$, where Y is a random variable denoting the number of floods exceeding the design flood in the n-year period. Likewise, risk is also defined as the probability that one or more floods (exceeding the design flood) will occur in the n-year period, i.e., $R = P(Y > 0) = 1 - P(Y = 0)$. Therefore, these probabilities can be also obtained using the binomial probability law (e.g., Mood et al. 1974).

The previously mentioned concepts, definitions, and equations related to return period T and hydrologic risk R have been commonly utilized in engineering practice, and are available in books and manuals (e.g., IACWD 1982; Chow et al. 1988; Bras 1990; Viessman and Lewis 2003). However, because of the growing awareness that changes in hydrologic extremes have been observed in many basins, there have been some attempts to apply nonstationarity concepts of extreme-value analysis, particularly for modeling extreme floods and sea levels (e.g., Coles 2001; El Adlouni et al. 2007; Villarini et al. 2009; Walter and Vogel 2010; Obeysekera et al. 2012; Cooley 2013). With the popularity of the generalized extreme value (GEV) distribution, some methods incorporate nonstationarity in the analysis by modeling the distributional parameters as a function of time or another variable, generally known as covariate, which may or may not be a function of time (Coles 2001). The covariate could be the changing land-use pattern or a climatic index such as Southern Oscillation Index (SOI), which may have an influence on the local extremes. Under nonstationary conditions the traditional definition of return period will not be applicable and the methods mentioned previously provide ways of computing a time-varying exceedance probability. Walter and Vogel (2010) defined a concept termed recurrence reduction factor and its use was demonstrated applying the log-normal probability distribution. Obeysekera and Park (2013) used nonstationarity concepts and the GEV for modeling sea-level extremes.

Furthermore, because of the concern on climate change during recent decades (Katz 1993), some key developments for extending the concepts of return period and risk associated with extreme events under nonstationary conditions have appeared primarily in the statistical and climate change literature (e.g., Wigley 1988, 2009; Olsen et al. 1998; Parey et al. 2007; Cooley 2009, 2013). However, they have received insufficient attention in the water resources literature. Some early work on the topic has been described by Wigley (1988, 2009), who presented a simple illustration on how nonstationarity may be considered in the traditional concepts of risk and uncertainty. Olsen et al. (1998) extended the concepts with a more rigorous mathematical treatment and derived the probability of the first failure in k years in addition to a risk formula applicable to nonstationary conditions. Olsen et al. (1998) has been unnoticed in the water resources literature (e.g., El Adlouni et al. 2007; Sivapalan and Samuel 2009; Walter and Vogel 2010; Obeysekera et al. 2012; Gilroy and McCuen 2012). Subsequently, Mandelbaum et al. (2007) developed the basis of nonhomogeneous geometric random variables, which paves the way for extending the concepts of return period and risk for nonstationary conditions. More recently, Cooley (2013) reviewed and compared the return period definitions suggested by Olsen et al. (1998) and Parey et al. (2007). Thus, current developments in modeling extreme events considering nonstationarity are sufficient to provide a rather simple unifying framework for applications in water resources engineering. Such a framework is presented in the next section.

Return Period and Risk under Nonstationarity

The probability distribution of annual floods is assumed as $F_Z(z, \underline{\theta}_t)$, where the parameter set $\underline{\theta}_t$ varies in accordance with time. It is also assumed that at an initial year, (e.g., year $t = 0$), a flood-related hydraulic structure has been designed (built) based on the flood quantile z_{q_0}, which corresponds to an initial return period $T_0 = 1/p_0 = 1/(1-q_0)$, where and p_0 and q_0 are the exceedance and nonexceedance probabilities of z_{q_0}, respectively. The assumption that the underlying model has parameters that vary through time may be viewed as if the flood distribution changes through the years (Fig. 2). In addition, the writers also assume that the occurrences of annual floods are independent. Thus, under such nonstationary condition the writers would like to evaluate the performance of the mentioned hydraulic structure using some basic metrics such as return period and risk; for this purpose the writers consider three conditions of nonstationarity, as follows: (1) increasing events, (2) decreasing events, and (3) random shifting events.

Case of Increasing Extreme Events

If extreme hydrologic events increase through time, it means that the exceedance probability of the floods affecting a flood-related hydraulic structure (which has a fixed capacity z_{q_0}) will also vary through time, i.e., $p_1, p_2, p_3, \ldots, p_t$. The sequence of p will be also increasing (Fig. 2). The time-varying p can be readily obtained from the assumed model as $p_t = 1 - q_t = 1 - F_Z(z_{q_0}, \underline{\theta}_t)$. Define the random variable X as the time at which a flood exceeding the design flood will occur for the first time. For example, the probability that the first flood exceeding the design flood z_{q_0} will occur at time $x = 1$ is p_1 and the probability that it will occur at time $x = 2$ is $(1-p_1)p_2$. In general, the probability that the first flood exceeding the design flood z_{q_0} will occur at time x is then given by

$$f(x) = P(X = x) = (1-p_1)(1-p_2)(1-p_3)\ldots(1-p_{x-1})p_x \qquad (5a)$$

$$f(x) = p_x \prod_{t=1}^{x-1}(1-p_t) \qquad x = 1, 2, \ldots, x_{\max} \qquad (5b)$$

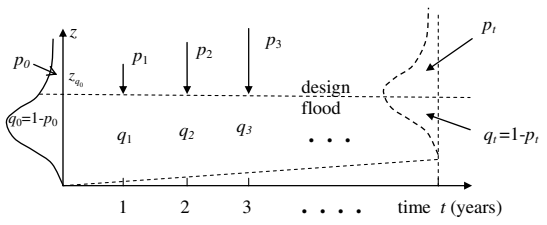

Fig. 2. Schematic depicting the design flood z_{q_0} in addition to exceeding (p_t) and nonexceeding ($q_t = 1 - p_t$) probabilities as they vary through years 1 to t (an illustration of nonstationary floods)

J. Hydrol. Eng. 2014.19:554-568.

where x_{max} = time at which $p = 1$. It is understood that in Eqs. (5*a*) and (5*b*) for $x = 1$, $f(1) = p_1$. Eqs. (5*a*) and (5*b*) are the probability distribution of the waiting time for the first flood to exceed the design flood, is a generalization of the geometric distribution that is applicable to nonstationary conditions, and has parameters (exceedance probabilities) varying in accordance with time. If the p values are the same (stationary condition), then the foregoing probability distribution simplifies to Eq. (2), the well-known geometric distribution as mentioned previously. A hypothetical example is included in a subsequent section to help distinguishing the difference between t and x in Eqs. (5*a*) and (5*b*) and other equations in this paper.

The CDF of the geometric distribution [Eqs. (5*a*) and (5*b*)] becomes

$$F_X(x) = \sum_{i=1}^{x} f(i) = \sum_{i=1}^{x} p_i \prod_{t=1}^{i-1}(1-p_t) = 1 - \prod_{t=1}^{x}(1-p_t)$$
$$x = 1, 2, \ldots, x_{max} \tag{6}$$

where $F_X(1) = p_1$ and $F_X(x_{max}) = 1$. Mandelbaum et al. (2007) introduced nonhomogeneous geometric random variables, which are similar to those in Eq. (6) and provide a convenient recursive formula for computing $f(x)$

$$p_x = \frac{f(x)}{1 - F(x-1)} \tag{7}$$

where $F(0) = 0$.

The writers assumed in Eqs. (5*a*), (5*b*), and (6) that the exceedance probability p increases continuously up to a point at which it becomes equal to 1. This may occur, for example, when the lower bound of the underlying distribution $F(z)$ becomes equal to z_{q_0} (as mentioned in the exponential example in a subsequent section of this paper.) In other cases the p may increase indefinitely, and in that case x_{max} in Eqs. (5*a*), (5*b*), and (6) will be infinity. Another possible scenario may be the case of an urbanizing catchment in which at year 1 it entered into a period of increasing floods lasting, for example, 25 years and thereafter, the flood events become stationary again but with a (limiting) probability of exceedance p_{25}. That is, from year 25 on the probabilities p_t in Eqs. (5*a*), (5*b*), and (6) will be constant and $x_{max} = \infty$. This case may be also viewed as an upward shift, although different than the random shifting extreme events that are considered in a subsequent section.

The previously mentioned geometric distribution under a nonstationary framework will enable determining the expected waiting time (return period) in which the flood exceeding the design flood z_{q_0} will occur for the first time

$$T = E(X) = \sum_{x=1}^{x_{max}} x f(x) = \sum_{x=1}^{x_{max}} x p_x \prod_{t=1}^{x-1}(1-p_t) \tag{8a}$$

$$T = E(X) = 1 + \sum_{x=1}^{x_{max}} \prod_{t=1}^{x}(1-p_t) \tag{8b}$$

where Eq. (8*b*) is a convenient simplification of Eq. (8*a*) in accordance with Cooley (2013).

Eqs. (8*a*) and (8*b*) gives the return period T for nonstationary conditions. This is consistent with the existing definition of return period for the stationary case. However, unlike the stationary case in which T is only a function of the exceedance probability p (a constant value), now in the nonstationary case T is a function of the time varying exceedance probabilities p_t. T is the first moment of the nonhomogeneous geometric distribution [Eqs. (5*a*) and (5*b*) are a function of parameters (i.e., the time-varying probabilities)]. Eqs. (8*a*) and (8*b*) have been derived relying on the geometric distribution [Eqs. (5*a*) and (5*b*)], which is applicable for nonstationary conditions. Olsen et al. (1998) derived the return period based on concepts of the binomial distribution and mentioned the possibility of using a nonhomogeneous Poisson process. Eq. (9) from Olsen et al. (1998) gives the probability that a failure first occurs in k years starting from year t (i.e., the probability varying in accordance with time) and Eq. (10) of Olsen et al. (1998) gives the return period that also varies in accordance with t. The main difference with the development in this paper is that the writers' procedure is based on the geometric distribution with varying parameters, it is easier to follow, the notation is simpler, and the derived return period is not a function of time.

The variance of X may be determined from $\text{var}(X) = E(X^2) - T^2$

$$E(X^2) = \sum_{x=1}^{x_{max}} x^2 p_x \prod_{t=1}^{x-1}(1-p_t) \tag{9}$$

The coefficient of variation of the waiting time variable X can then be determined as $\eta(X) = \sigma(X)/T$, where $\sigma(X)$ is the standard deviation of X.

Likewise, the risk of failure of the mentioned hydraulic structure having design life n may be determined by $R = \text{P}(X \le n) = F_X(n)$, such that from Eq. (6)

$$R = \sum_{x=1}^{n} p_x \prod_{t=1}^{x-1}(1-p_t) = 1 - \prod_{t=1}^{n}(1-p_t) \tag{10}$$

and the reliability becomes

$$R_\ell = \prod_{t=1}^{n}(1-p_t) \tag{11}$$

The reliability of the structure is also equivalent to the probability that no floods exceeding the design flood will occur in the n-year period. For example, for $n = 2$, $R_\ell = (1-p_1)(1-p_2)$. Eq. (11) then gives R_ℓ in general for any value of n. Eq. (10) reduces to Eq. (3), the well-known equation of the risk of failure $R = 1 - (1-p)^n$ in the case that the p values are constant (stationary condition). Another major difference between the derivation reported in this paper with that of Olsen et al. (1998) is that it arises readily from the CDF of the geometric distribution [Eq. (6)], whereas the equation of Olsen et al. (1998) was derived from the CDF of the $\max(Z_1, Z_2, ..., Z_n)$.

Case of Decreasing Extreme Events

In some cases, extreme events may exhibit a decreasing trend; consequently, the exceedance probability p_t will also decrease through time. This may occur, for example, with extreme sea levels. In some locations, the uplift of the surrounding land due to tectonic activity may be larger than the global sea-level rise and consequently the relative sea level (measured with respect to a local datum) may actually decrease in accordance with time. In such cases, extreme local sea-levels will also decrease. The writers present some equations that are minor modifications of those mentioned previously

$$f(x) = p_x \prod_{t=1}^{x-1}(1-p_t) \qquad x = 1, 2, \ldots, \infty \tag{12a}$$

J. Hydrol. Eng. 2014.19:554-568.

$$T = E(X) = \sum_{x=1}^{\infty} x p_x \prod_{t=1}^{x-1}(1 - p_t) \tag{12b}$$

$$E(X^2) = \sum_{x=1}^{\infty} x^2 p_x \prod_{t=1}^{x-1}(1 - p_t) \tag{12c}$$

In some cases of decreasing extreme events one may conceive the use of a probability distribution with an upper bound and in such cases there may be a limiting time x in which the p_x reaches the value of zero. In cases for which extreme events such as low flows have a decreasing trend (thus increasing the nonexceedance probability q), a future scenario may be that such decreasing low flows will eventually converge exponentially to a constant (although it may be conceivable that because of extreme human activities and climate change the low flows may become zero). The risk and reliability formulas [Eqs. (10) and (11)] remain the same.

Case of Shifting Extreme Events

In some situations, natural climate variability may occur in the form of shifting regimes that may be of random lengths (e.g., Boes and Salas 1978; Sveinsson et al. 2003; Kiem et al. 2003; Sveinsson et al. 2005; Enfield and Cid-Serrano 2006; Rao 2009; Villarini et al. 2009a; Park et al. 2011). The shifts may be reflected in one or more parameters of the probability distribution of extremes. For example, in cases of extreme floods a common situation is when the mean of the floods shifts randomly over one or more levels (e.g., Sveinsson et al. 2005). However, if the shifts are of decadal or multidecadal nature, typical observational records may not have sufficient shifts to determine the probabilistic characteristics of the duration of shifts. For example, the AMO, which has been linked to rainfall regimes (Enfield et al. 2001) and floods (Rao 2009), has only a few shifts in its observational data set, which begins in the year 1856. Sveinsson et al. (2005) applied a shifting mean model and the geometric distribution to estimate the shift lengths, and employed the autocorrelation function of the sample data to estimate the corresponding parameters. To estimate the return period and risk using the mentioned shifting mean model, data generation was employed (Sveinsson et al. 2005). Enfield and Cid-Serrano (2006) used a 450-year proxy tree-ring data set to study the AMO shifts and fitted a gamma distribution, which was in turn used to compute the probability of a future shift given the length of a current AMO regime. Park et al. (2011) demonstrated the use of this approach for predicting storm surge extremes assuming that the extreme value distributions depend on the AMO regime. One of the major challenges in dealing with shifting extremes is the estimation and projections of regime shifts.

The writers assume that, in general, the extreme events are modeled by k regimes and the probabilities of each regime can be estimated from either the observational records or proxy data. The nonexceedance probability in any given year can then be expressed as

$$F_Z = \sum_{j=1}^{k} \alpha^j F_Z^j \tag{13}$$

where α^j = probability of being in regime j at any time; and F_Z^j = nonexceedance probability (of the underlying variable) corresponding to the distribution associated with regime j, i.e., $\sum_{j=1}^{k} \alpha^j = 1$. Once F_Z and consequently p_x are computed, the expressions provided in the preceding sections can be used to compute $T = E(X)$ and R. Further details of the procedure will be described in the Applications section.

Examples

The writers provide in this section some examples that may help understanding and applying the equations for estimating the return period and risk under nonstationary conditions as described previously. First, a hypothetical example is included to demonstrate the computations involved in estimating T and R for nonstationary conditions and compare the results with those for stationary conditions. A more realistic yet simple example using the exponential distribution is then described next, in which a trend in the scale parameter is assumed.

Hypothetical Example

This hypothetical example considers the case in which the exceedance probabilities decrease linearly for the first 5 years and then become constant for the future years (Table 1), i.e., $p_1 = 0.2$, decreasing linearly to $p_5 = 0.1$, then remains at 0.1 for $t > 5$ (Table 1 shows values through $t = 15$) and $x_{\max} = \infty$. Because the p values decrease in accordance with time one would expect that the return period would be bigger relative to that of the stationary case. The probability distribution of the waiting time is determined from Eqs. (5*b*), third column (Table 1). The fourth column (Table 1) gives the elements of the summation terms in Eq. (12*b*), and the return period is determined from Eq. (12*b*), bottom (Table 1). It gives a return period equal to $T = 7.9$ years for the nonstationary condition of decreasing values of p. If the exceedance probability of the year 1 had remained constant through the years (the stationary case), then the return period would be $T = 1/0.2 = 5$ years [in this case Eq. (2) will apply instead of Eqs. (5*b*) and $T = 1/p$ instead of Eq. (12*b*)]. Likewise, one would expect that the risk of failure will decrease compared to the stationary case. For example, Table 1 shows that for $n = 5$ years the risk is about 0.56, whereas the risk for the stationary case is equal to $R = 1 - 0.8^5 = 0.67$.

Table 1. Hypothetical Example for Determining the Return Period T and Risk R for Exceedance Probabilities Decreasing for the First 5 Years and Thereafter Remaining Constant

Time t/x	Exceedance probability p_t/p_x	$P(X = x)$ Eq. (5*b*)	$xP(X = x)$	Design life n	Risk Eq. (10)	Reliability Eq. (11)
1	0.200	0.2000	0.200	1	0.2	0.8
2	0.175	0.1400	0.280	2	0.34	0.66
3	0.15	0.0990	0.297	3	0.439	0.561
4	0.125	0.0701	0.2805	4	0.509	0.491
5	0.1	0.0491	0.2454	5	0.558	0.442
6	0.1	0.0442	0.2651	6	0.602	0.398
7	0.1	0.0398	0.2783	7	0.642	0.358
8	0.1	0.0358	0.2863	8	0.678	0.322
9	0.1	0.0322	0.2899	9	0.710	0.290
10	0.1	0.0290	0.2899	10	0.739	0.261
15	0.1	0.0171	0.2567	15	0.846	0.154
∞	0.1	$\Sigma = 1.00$	$T = \mathrm{E}(X) = 7.9$ Eq. (12*b*)	∞	1.0	0.0

Note: For distinguishing t and x in the first two columns in Table 1 in addition to Eqs. (5*b*) and (12*b*), let $x = 4$, for which $p_x = p_4 = 0.125$. The exceedance probabilities for $t = 1, 2, 3, 4$ are $p_1 = 0.2$, $p_2 = 0.175$, $p_3 = 0.15$, and $p_4 = 0.125$. Therefore, Eq. (5*b*) gives $f(4) = P(X = 4) = (1 - 0.2) \times (1 - 0.175) \times (1 - 0.15) \times 0.125 = 0.0701$.

Exponential Distribution

The writers use a time-varying exponential distribution, which may be represented by the CDF as

$$F_Z(z) = 1 - \exp(-\lambda_t z) \tag{14}$$

where the scale parameter $\lambda_t > 0$ is assumed to be a function of time t. Considering that at time $t = 0$ a design has been made using a return period $T_0 = 1/p_0 = 1/(1 - q_0)$, the design quantile z_{q_0} can be determined from Eq. (14) as $p_0 = 1 - q_0 = \exp(-\lambda_0 z_{q_0})$. Likewise, the time-varying exceedance probability of the quantile z_{q_0} is given by $p_t = \exp(-\lambda_t z_{q_0})$. For illustration, the writers assume that $\lambda_t = \max(0, \lambda_0 - at)$, where the parameter a is the rate of change in λ_t. For $t \le \lambda_0/a$

$$p_t = \exp(-\lambda_0 z_{q_0}) \exp(atz_{q_0}) = p_0 \exp(atz_{q_0}) \tag{15}$$

and $p_t = 1$ for $t > \lambda_0/a$. Additionally, $p_t = 1$ for $t = (1/az_{q_0})\ln(1/p_0)$. Thus, this is a case in which the exceedance probability p increases continuously as time t increases up to a maximum value $p_t = 1$. The writers will then apply Eq. (8*a*), where $x_{\max} = (1/az_{q_0})\ln(1/p_0)$ to find the return period T and Eq. (10) to determine the risk R.

To illustrate the reduction in return period T due to nonstationarity, the writers consider $\lambda_0 = 0.5$ and three cases of a = (0.0001, 0.001, 0.005). For example, for $T_0 = 20$, $p_0 = 0.05$, $q_0 = 0.95$, $z_{q_0} = z_{0.95} = 5.99$, and $a = 0.005$, Eq. (15) can be used to determine $p_1 = 0.0515$, $p_2 = 0.0531$, and so on, and $p_t = 1$ for $t = 100$, i.e., $x_{\max} = 100$. Those values are then entered into Eq. (8*a*) to determine the return period T for nonstationary conditions. Fig. 3 shows the variation of the return period T, identified as nonstationary T (in the y-axis of Fig. 3) as a function of the initial design return period T_0 (stationary T in the x-axis of Fig. 3) for the assumed three cases of rate of change in λ_t. From this illustrative example, the reduction in T is significant particularly for larger values of the rate of change a. For example, if the original design corresponds to a 100-year return period, the actual return periods under nonstationary conditions of varying λ are 91, 60, and 31 years, respectively, for the three cases considered previously. The reduction of T is larger for projects with a higher level of protection. As a consequence, if a project is to have, for example, a 50-year level of protection under nonstationary conditions over the life of the facility, the initial design may have to be much larger. For example, if $a = 0.001$, the project will need to be designed for

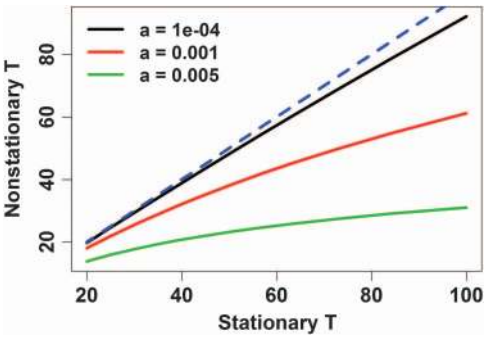

Fig. 3. (Color) Nonstationary T as a function of the initial design return period T_0 (denoted as stationary T in the x-axis) for the exponential distribution with $\lambda_0 = 0.5$ and three cases of trends in λ for a = (0.0001, 0.001, 0.005); the dashed line is the 45° line for comparison with the three curves to demonstrate the extent of reduction in T

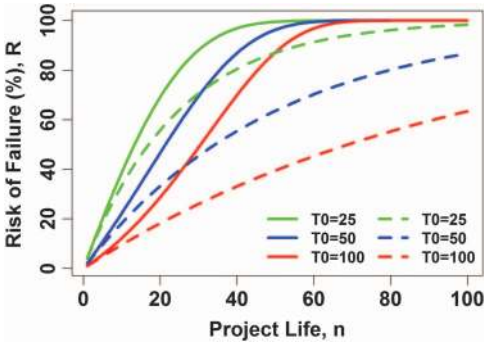

Fig. 4. (Color) Nonstationary risk of failure R of Eq. (10) as a function of project life n for the exponential distribution with $\lambda_0 = 0.5$; initial designs for $T_0 = 25$, 50, and 100 years; trend in λ with $a = 0.005$; the dashed and solid lines represent the stationary and nonstationary cases, respectively

about a 75-year initial return period to ensure a 50-year level of protection over the life of the project.

The hydrologic risk of failure under nonstationary conditions can also be illustrated using Eq. (10). Fig. 4 shows the increase in risk for $\lambda_0 = 0.5$, $a = 0.005$, and three cases of initial designs, i.e., $T_0 = 25$, 50, and 100. The dashed-lines in Fig. 4 show the risk for the stationary condition from Eq. (3), whereas the solid lines give the risk for the nonstationary conditions using Eq. (10). For any given value of n the risk under nonstationary conditions is bigger than that for stationary conditions. The risk increase due to nonstationarity is larger for a higher initial level of protection (i.e., higher T_0). Moreover, depending on the project life and initial level of protection, a project life for which the risk of failure is 100% may be much shorter in duration, as shown by the solid lines approaching 100% much more quickly (Fig. 4). If the risk of failure is to be maintained as in the stationary case, the project may have to be designed for a much higher initial level of protection under nonstationarity.

Applications

The writers include in this section some applications for determining the return period T and hydrologic risk R for nonstationary conditions based on some actual data of extreme floods and extreme sea-levels that show increasing or decreasing trends and shifting patterns. The applications are based on the GEV distribution with time-varying parameters. The GEV has the advantage that future nonstationarity can be included explicitly by using time-dependent parameters. The cumulative distribution function of the GEV may be expressed as in Coles (2001) and Katz (2013)

$$F(z, \underline{\theta}_t) = \exp\left\{-\left[1 + \varepsilon\left(\frac{z - \mu_t}{\sigma_t}\right)\right]^{-1/\varepsilon}\right\} \tag{16}$$

where $\underline{\theta}_t = \{\mu_t, \sigma_t, \varepsilon\}$ represents the parameter set in which μ_t and σ_t are the time-dependent location and scale parameters, respectively; ε is the shape parameter; and $[1 + (\varepsilon/\sigma_t)(z - \mu_t)] > 0$. When $\varepsilon \to 0$, Eq. (16) reduces to the Gumbel distribution

$$F(z, \underline{\theta}_t) = \exp\left[-\exp\left(-\frac{z - \mu_t}{\sigma_t}\right)\right] \tag{17}$$

The nonstationarity in extreme variables, such as extreme sea-levels and extreme floods, may be modeled by assuming that

J. Hydrol. Eng. 2014.19:554-568.

both the location parameter μ and scale parameter σ are time-dependent (e.g., El Adlouni et al. 2007; Menendez and Woodworth 2010). Commonly the location parameter μ is assumed to vary in accordance with time but if the upper bound of the annual maxima may also increase in accordance with time, then in such cases the scale parameter may have to be modeled as a function of time. Some examples are $\mu_t = \mu_0 + at$ and $\log \sigma_t = \sigma_0 + bt$ (Ruggiero et al. 2010; Katz 2013). The parameters can also be modeled as functions of exogenous variables as covariates. The shape parameter ε is difficult to estimate reliably and for this reason it is normally modeled as a constant (Coles 2001; Katz 2013). Typically, the length of the underlying data (e.g., annual floods) may not be long enough to reliably estimate all the parameters as time-dependent. The computations using the GEV model with trends were performed with the R-package *extRemes* (Guilleland and Katz 2011).

The significance of the trend in the parameters (e.g., trend in the location parameter μ) may be evaluated using the likelihood ratio test (Coles 2001), which uses the deviance statistic $D = 2\{\ell(M_r) - \ell(M_s)\}$, where $\ell(M_r)$ and $\ell(M_s)$ are the log-likelihood functions of the fitted models M_r (e.g., with a linear trend in the parameter μ) and M_s (without a trend in the parameter), respectively; and r and $s(r > s)$ are the number of parameters in the models considered. The test of the validity of one model against the other is based on the probability distribution of D, which is approximately chi-square distributed with $r - s$ degrees of freedom. For example, consider comparing model $M_3 = \{\mu, \sigma, \varepsilon\}$, i.e., a model with three parameters without trends, versus model $M_4 = \{\mu_0 + at, \sigma, \varepsilon\}$, a model with four parameters with a trend in the location parameter μ. Under the null hypothesis that $a = 0$, the statistic D is approximately chi-square distributed with $4 - 3 = 1$ degree of freedom and one must reject model M_3 in favor of M_4 if $D > \chi^2_{1-\alpha}(1)$, where $\chi^2_{1-\alpha}(1)$ is the $1 - \alpha$ quantile of the chi-square with 1 degree of freedom and α is the significance level. As suggested by Katz (2013), one may apply the Akaike's information criteria (AIC) to compare among competing models, where $\mathrm{AIC}(k) = 2[-\ell(M_k) + k]$ for a model with k parameters. For example, $k = 3$ for the GEV model with no trend and $k = 4$ for the model with a linear trend in μ. The model that is preferred is that having the minimum value of AIC. The test based on the deviance statistic and the model selection based on AIC do not give information about the goodness-of-fit, and thus the performance of the selected model is generally assessed by inspecting diagnostic plots such as the probability and quantile plots (Coles 2001).

The design-quantile at time $t = 0$ based on the GEV may be obtained from Eq. (16) as

$$z_{q_0} = \mu_0 - \frac{\sigma_t}{\varepsilon}\{1 - [-\ln(1 - p_0)]^{-\varepsilon}\} \tag{18}$$

When $\varepsilon \to 0$, the corresponding expression for the Gumbel model is

$$z_{q_0} = \mu_0 - \sigma_t \ln[-\ln(1 - p_0)] \tag{19}$$

Likewise, the expression for the time-varying exceedance probability p_t relative to the design quantile z_{q_0} for the case where $\varepsilon \neq 0$ is obtained from Eq. (16)

$$p_t = 1 - \exp\left\{-\left[1 + \varepsilon\left(\frac{z_{q_0} - \mu_t}{\sigma_t}\right)\right]^{-1/\varepsilon}\right\} \tag{20}$$

whereas for $\varepsilon \to 0$ the expression for p_t is obtained from Eq. (17) as

$$p_t = 1 - \exp\left[-\exp\left(-\frac{z_{q_0} - \mu_t}{\sigma_t}\right)\right] \tag{21}$$

Increasing Floods

In many urbanizing watersheds, annual flood peaks are increasing due to continuous land-use changes. In such situations project designs will need to consider nonstationarity in the probability distribution of flood peaks. The writers provide the application of the return period and risk concepts for nonstationary conditions, as outlined in previous sections, to two drainage basins, as follows: (1) Aberjona River Basin at Winchester, Massachusetts (Vogel et al. 2011); and (2) Little Sugar Creek at Archdale Drive in Charlotte, North Carolina (Villarini et al. 2009b) by using the GEV distribution. Ng and Vogel (2010) describes the land-use changes in the Aberjona River leading to the increasing flood data, which were analyzed by Vogel et al. (2011) to investigate the changes in the return period in the future. Villarini et al. (2009b) describes the nonstationarity in the probability distribution of annual flood peaks for the Little Sugar Creek due to rapid urbanization in Charlotte.

Fig. 5 shows the plots of annual flood peaks for both the Aberjona River and Little Sugar Creek basins. In both cases the flood magnitude and variability appear to be increasing in accordance with time. For the Aberjona River various combinations of GEV models with and without trends in the location, scale, and shape parameters were tested and compared based on deviance and AIC statistics as described previously. The GEV models with shape parameter $\varepsilon \neq 0$ were better than GEV with $\varepsilon = 0$, i.e., a Gumbel model. Based on the model-selection criteria described previously, GEV models that included a trend in the shape parameter were inferior than those with a constant shape parameter. The writers

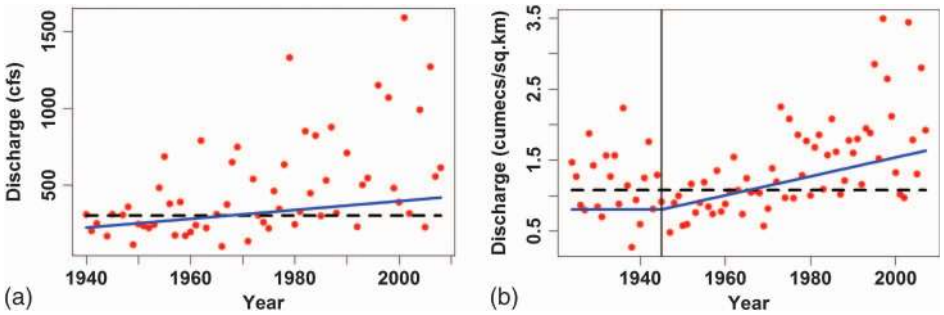

Fig. 5. (Color) Flood peaks [in both cases the trend lines for the location parameter (solid blue line) and the fitted value without the trend (dashed black line) are shown]: (a) Aberjona River Basin; (b) Little Sugar Creek Basin

J. Hydrol. Eng. 2014.19:554-568.

Table 2. Stationary and Nonstationary GEV and Gumbel Models Fitted to the Annual Flood Data of Aberjona River and Little Sugar Creek

Flood data, basin	Fitted model	Estimated parameters and standard errors[a]	Log-likelihood	Test statistics[b]
Aberjona River	Stationary GEV	$\mu = 301.8,\ 25.5\ \sigma = 170,\ 22.3$ $\varepsilon = 0.354,\ 0.129$	$\ell(M_3) = -415$	$D = 8.07\ \chi^2 = 3.84\ p$–value $= 0.004$ AIC(3) = 835.9 AIC(4) = 829.8
	Nonstationary GEV	$\mu_0 = 319.4,\ 25.4\ a = 2.88,\ 1.02$ $\sigma = 163.4,\ 21.2\ \varepsilon = 0.304,\ 0.133$	$\ell(M_4) = -410.9$	
Little Sugar Creek	Stationary Gumbel	$\mu = 1.08,\ 0.05\ \sigma = 0.46,\ 0.04$	$\ell(M_2) = -67.81$	$D = 25.0\ \chi^2 = 3.84\ p$–value $= 5.77 \times 10^{-7}$
	Nonstationary Gumbel[c]	$\mu_0 = 1.118,\ 0.045\ a = 0.012,\ 0.002$ $\sigma = 0.396,\ 0.034$	$\ell(M_3) = -55.31$	AIC(2) = 139.6 AIC(3) = 116.6
	Nonstationary Gumbel[d]	$\mu_0 = 1.118,\ 0.046\ a = 0.133,\ 0.002$ $\sigma_0 = -0.943,\ 0.087\ b = 0.008,\ 0.004$	$\ell(M_4) = -53.17$	$D = 4.28\ \chi^2 = 3.84\ p$–value $= 0.0386$ AIC(4) = 114.3

[a]Standard errors are shown after the parameter values.
[b]χ^2 = chi-square statistic.
[c]With trend in location parameter only.
[d]With trends on both location $\mu_t = \mu_0 + at$ and scale $\ln\ \sigma_t = \sigma_0 + bt$.

had to choose between a GEV model having trends in both the location and scale parameters versus a GEV model with a trend in the location parameter only. For the purpose of illustrating the results to be obtained for T and R for this river, the writers selected the simpler model because it gave comparable diagnostic plots. Thus, the details described next refer to results for the GEV model with a time-varying location parameter $\mu_t = \mu_0 + at$ and constant scale and shape parameters. For comparison, results shown in Table 2 also include the GEV model with constant parameters. The estimated GEV parameters without trend gave $\mu = 301.8$ cfs, $\sigma = 170$ cfs, and $\varepsilon = 0.354$, whereas the estimates with trend gave $\mu_t = (319.4 + 2.88\ t)$ cfs, $\sigma = 163.4$ cfs, and $\varepsilon = 0.304$. The corresponding log-likelihood values are $\ell(M_3) = -415$ and $\ell(M_4) = -410.9$, respectively. The likelihood ratio test statistic D for comparing the two models with and without trend in μ_t is 8.07, which is significant at the 5% level based on the chi-square distribution with one degree of freedom. In addition, AIC(3)=835.9 and ACI(4)=829.8, which confirm that the GEV model with a trend in the location parameter is preferred over the model without a trend. Fig. 6 shows the residual diagnostic plots (probability and quantile plots), which justifies selecting a GEV model with trend

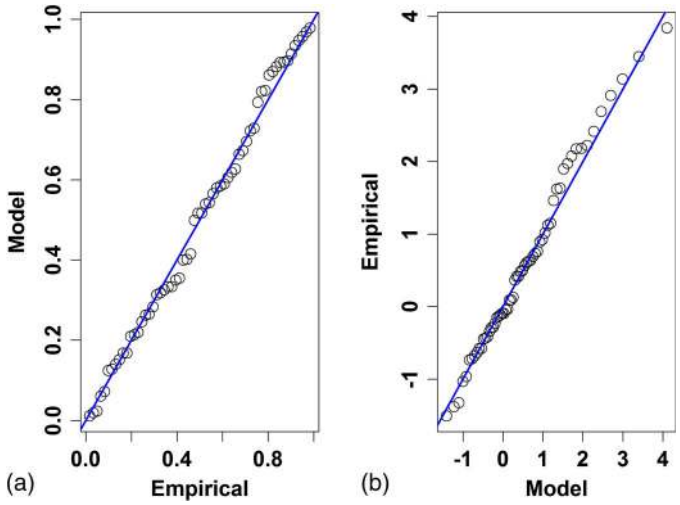

Fig. 6. Residual diagnostic plots for the GEV model with linear trend in the location parameter for the Aberjona River flood data: (a) residual probability plot; (b) residual quantile plot (using Gumbel as the reference distribution)

in the location parameter in addition to constant scale and shape parameters. Table 2 summarizes the estimated parameters along with their standard errors and the test statistics.

For the flood data at Little Sugar Creek, various combinations of GEV models were tested and compared. The results based on the D test and AIC, as described previously, suggested that the GEV models with shape parameters $\varepsilon \neq 0$ were no better than GEV models with $\varepsilon = 0$, i.e., the Gumbel model. Gumbel models with trend in the location or in the scale parameters and trend in both parameters were tested. Overall, a Gumbel model with trends in both parameters gave better results based on the D test and AIC as well as diagnostic plots. Early periods in the Little Sugar Creek flood record [Fig. 5(b)] do not show increasing floods; the writers then assumed that prior to 1945, the location parameter was constant. Regarding the modeling of the annual flood peaks of Little Sugar Creek, Villarini et al (2009b) conducted a detailed study by using the generalized adaptive models for location, scale, and shape (GAMLSS) parameters, which was quite versatile for modeling nonstationary processes. A number of relevant issues were examined such as the relationship between population trends and flood frequency as well as the effects of trends in annual maximum rainfall. Villarini et al. (2009b) also suggested the need of developing alternative definitions of return period to deal with nonstationary flood data.

Fig. 5 also shows for the two mentioned basins the time-varying location parameters. The time-varying exceedance probability p_t is determined from Eq. (20) for Aberjona River and Eq. (21) for Little Sugar Creek, given the initial design flood quantiles z_{q_0} corresponding to specified return periods T_0. The return periods T for the nonstationary cases are then computed using Eq. (8*a*), where $x_{\max} = \infty$. Fig. 7 shows the variation of T as a function of T_0 for both cases. In computing the return period (and the corresponding risk) for future conditions, anticipated variation of μ_t needs to be assumed. In the case of rapid urbanization development, μ_t may increase up to some given time in the future followed by a constant value representing the built-out of the basin. Alternatively, one may assume that μ_t continues increasing indefinitely at the same pace (e.g., linear increase) or at a different rate of increase. Planners need to evaluate such possible future rates of development that may take place in the basin.

Fig. 7 shows that for both cases the nonstationary return period T is smaller than the stationary return period T_0. For example, for $T_0 = 50$ years, $T = 40.7$ years for Aberjona River and $T = 22$ years for Little Sugar Creek. The reason for the bigger differences in the return period for Little Sugar Creek is because the trend

J. Hydrol. Eng. 2014.19:554-568.

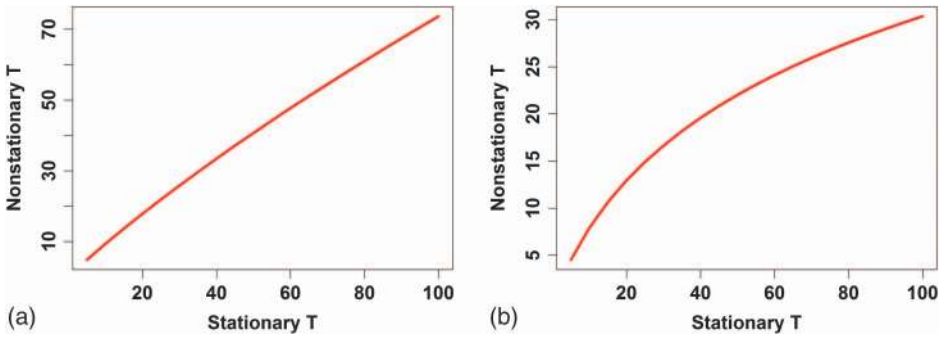

Fig. 7. (Color) Variation of the nonstationary return period T as a function of the initial return period T_0 (termed stationary T in the x-axis): (a) Aberjona River Basin; (b) Little Sugar Creek Basin

in the floods is bigger than for Aberjona River. These curves may be used to make design decisions in case of nonstationary flood regimes resulting from rapid urbanization or climate change. For example, in case of the Aberjona River, to ensure a level of protection equal to $T = 50$ years over the life of a project one may have to use an initial design that has a level of protection of about $T_0 = 65$ years [Fig. 7(a)]. In the case of Little Sugar Creek, the corresponding initial T_0 will have to be as high as 435 years to ensure that $T = 50$ years under nonstationary conditions.

This difference between the two examples is also reflected in the resulting risk of failure (Fig. 8). Under stationary conditions, the risk of failure R increases in accordance with project life n (dashed lines in Fig. 8). However, due to nonstationarity, the risk of failure over the project life will increase as shown by the solid lines (Fig. 8) for the three cases of initial design. The R for nonstationary conditions is bigger than the R for stationary. For example, for Little Sugar Creek with an initial return period $T_0 = 100$ years and design life $n = 50$ years, the risks are 39.5 and 88% for stationary and nonstationary conditions, respectively [Fig. 8(b)]. For the reasons explained previously, the increase in risk of failure for Little Sugar Creek is higher compared to that of the Aberjona River, particularly for projects requiring a higher level of protection [compare the curves for $T_0 = 25$ years versus $T_0 = 100$ years (Fig. 8)]. These risk curves (Fig. 8) may be used for making design decisions for projects experiencing nonstationary conditions.

Increasing and Decreasing Sea Level Extremes

Design of coastal infrastructure requires the estimation of extreme sea-level at project locations. Global average sea level has been rising at the rate of 1.7 mm/year since the middle of the nineteenth century (Church and White 2011). Historically, the sea level extremes have increased along with the increase in mean sea levels at locations along the coasts. Although the historical tide-gage data show little or no acceleration (Houston and Dean 2011; Watson 2011), it is expected that the global mean sea level will be increasing at a faster rate during the 21st century and beyond (Bindoff et al. 2007; Houston 2012) and as a consequence sea-level extremes will also change. However, the projections of the future sea-levels are highly uncertain, which have led coastal engineering specialists to suggest scenario-based approaches for mean sea-level increase (NRC 1987; USACE 2011; Obeysekera and Park 2013).

Sea level at a particular coastal location, the relative sea level (RSL), is the result of both the global change as well as the vertical land movement at that location. At some locations, although the global component is increasing, actual RSL may decrease due to such reasons as tectonic uplift. However, at locations where land subsidence is significant, RSL is larger than the global rate. Because RSL is what is important for the planning and design of coastal projects, future variations of RSL extremes are important and need to consider nonstationarity due to sea-level rise acceleration.

Obeysekera and Park (2013) demonstrated that the RSL extremes can be modeled by using a GEV with time-varying parameters. A particular case is when only the location parameter μ_t is a function of time and the other two parameters are assumed to be constants. Using the tide-gage data along the coast of the United States, it was demonstrated that μ_t can be modeled with a fixed offset e with respect to the mean sea level. Assuming that the

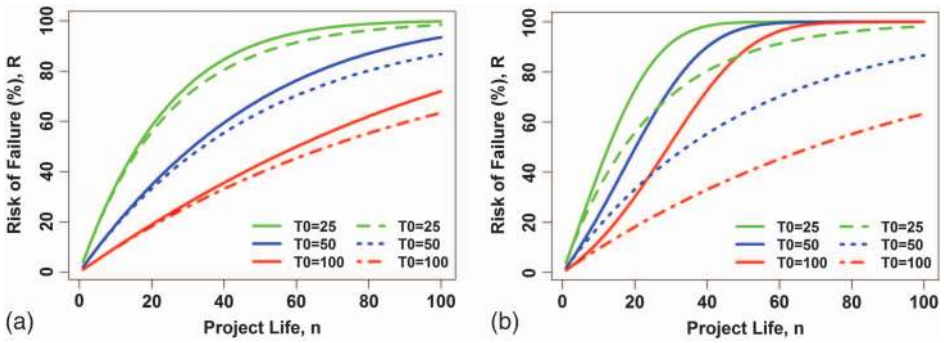

Fig. 8. (Color) Nonstationary risk of failure as a function of project life n (assuming initial designs for $T_0 = 25$, 50, and 100 years; the dashed lines show the risk for the stationary condition, whereas the solid lines show the risk for nonstationary conditions): (a) Aberjona River Basin (assuming the GEV model); (b) Little Sugar Creek Basin (assuming the Gumbel model)

J. Hydrol. Eng. 2014.19:554-568.

variation is quadratic, the future mean relative sea level variations may be represented as

$$\mu_t = ct + bt^2 + e \tag{22}$$

where t = time; the coefficient c incorporates the linear contributions of global sea level rise and the local component; parameter b = rate of acceleration in sea level trend; and parameter e = offset from the mean sea level (USACE 2011). Using Eq. (22), the writers demonstrate an application of nonstationary return period and risk concepts for two locations, as follows: (1) Key West, Florida, where sea levels are increasing; and (2) Adak, Alaska, where the mean sea-level is decreasing due to uplift. The values of b, the quadratic coefficient of the global sea-level acceleration, are future sea-level rise scenario dependent. USACE (2011) in a national guidance document included three scenarios termed "modified NRC-I, II, and III," with b values equal to 2.71×10^{-5}, 7×10^{-5}, and 11.3×10^{-5}, respectively. For illustration the writers use in this paper the NRC-I, i.e., $b = 2.71 \times 10^{-5}$.

Fig. 9 shows the mean and annual maxima of RSL for Key West, which is characterized by increased sea levels, and Adak, where relative sea level has been declining due to uplift. Fig. 9 also shows the fitted linear trends for mean sea-level and the time-varying location parameters μ_t for each location. Historic data do not show a quadratic variation in sea level and consequently lacks significant acceleration. Therefore, the writers fitted a linear regression to obtain the offset parameter. However, as explained previously, future mean sea-level rise rate is expected to accelerate, which is why a quadratic equation is used for future applications. Summarizing, the GEV parameters used for the RSL extremes are $c = 2.32$ mm/year, $b = 2.71 \times 10^{-5}$, $e = 552$ mm, $\sigma = 52.56$ mm, and $\varepsilon = 0.199$ for the Key West gage, and $c = -1.34$ mm/year, $b = 2.71 \times 10^{-5}$, $e = 1{,}079$ mm, $\sigma = 111.3$ mm, and $\varepsilon = -0.26$ for the Adak gage. In both cases diagnostic checks were performed using the probability and quantile plots (as described previously), and the results were acceptable. Using these parameters, the nonstationary return period and the risk were computed using the equations and methods derived previously.

Fig. 10 shows the comparison of the nonstationary return period T versus the stationary return period T_0 for both cases analyzed. The reduction of return period T as a function of T_0 [Fig. 10(a)] is consistent to that of increasing floods and it can be significant. However, the variation of the return period T for Adak is different, i.e., the nonstationary T is bigger than that for stationary up to about 40 years and thereafter the nonstationary T becomes smaller. The reason is that for Adak there is a decreasing sea-level [Fig. 10(b)], but as indicated previously, because of the quadratic term in Eq. (22), eventually the sea level will increase in accordance with time and that explains the behavior of T [Fig. 10(b)]. The risk as a function of the project life n under nonstationary conditions is compared versus the risk for stationary conditions for the cases of project designs given by $T_0 = 25$, 50, and 100 years (Fig. 11). In the case of Key West, where the RSL increases in accordance with time (and consequently the exceedance probability p_t also increases), the nonstationary risk for a given value of n is consistently bigger than that for stationary conditions. The nonstationary risk may approach to 100% for n less than 80 years [Fig. 11(a)]. However, in the case of Adak, where the RSL decreases in accordance with time [Fig. 9(b)], the risk for nonstationary conditions is actually smaller than the risk for stationary conditions, at least for values of n of about 80 years, but thereafter the nonstationary risk becomes bigger [Fig. 11(b)] because of the quadratic term in Eq. (22), which eventually will make the RSL increase as time increases. The cases described previously illustrate that generally risk

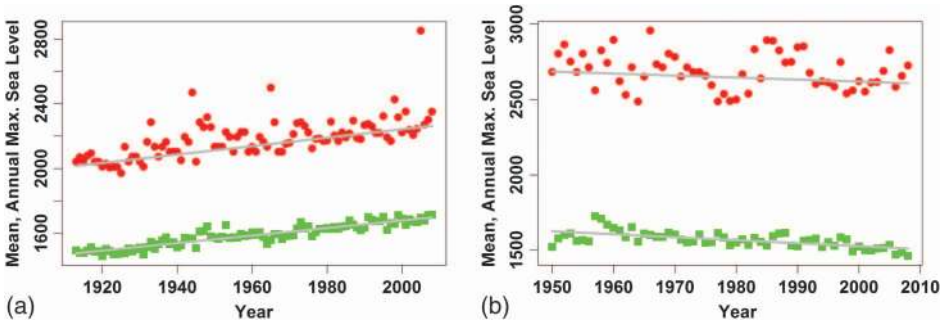

Fig. 9. (Color) Mean sea level and annual maxima [also shown are the fitted linear regression line for mean sea level and the linear time trend for the location parameter; the offset parameter e in Eq. (22) is estimated to be the mean difference between these two lines]: (a) Key West, Florida (increase); (b) Adak, Alaska (decrease)

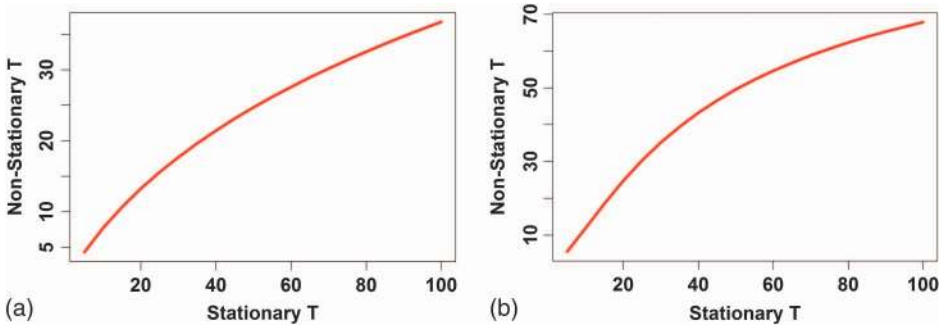

Fig. 10. (Color) Reduction in return period T as a function of T_0: (a) Key West extreme RSL; (b) Adak extreme RSL

J. Hydrol. Eng. 2014.19:554-568.

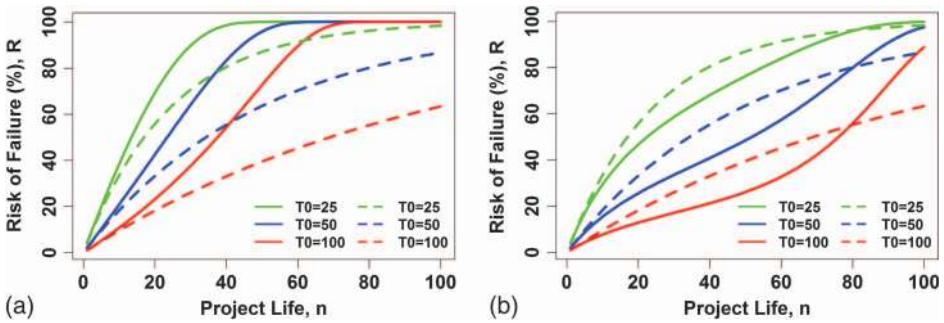

Fig. 11. (Color) Increase in risk of failure R as a function of project life n (the dashed lines show the risk for the stationary condition, whereas the solid lines show the risk for nonstationary conditions): (a) Key West; (b) Adak

of failure for nonstationary conditions exceeds that for stationary situations, although in cases such as Adak the counteracting effects of decreasing sea levels due to upward movement of land elevation is balanced by the accelerating global sea-level rise of the modeled scenario.

Shifting Floods

Peak flood regimes in some river basins are influenced by multiple climatic regimes, each of which may last for several years or even decades. Examples of shifting flood-records may be found in basins that are influenced by teleconnections to such phenomena as the ENSO, AMO (Enfield et al. 2001), and PDO (Mantua et al. 1997). In this example, the writers illustrate an application of the return period and risk concepts to the case of shifting floods associated with the St. Johns River Basin near Christmas, Florida. In a discussion by Rao (2009) on a paper by Griffis and Stedinger (2007), two distinct regimes were identified for floods in the St. Johns River that appear to be related to the AMO, which has long periods of shifting patterns that affect the climate of the Florida peninsula (Enfield et al. 2001; Trimble et al. 2006). Based on the work of Rao (2009), the writers identified two periods spanning 1944–1969 and 1970–1997 corresponding to warm and cold periods of the AMO.

With two shifting regimes, i.e., $k = 2$ in Eq. (13), the flood data in the St. Johns River are in accordance with a mixed distribution (e.g., Waylen and Caviedes 1986)

$$F_Z = \alpha^1 F_Z^1 + (1 - \alpha^1) F_Z^2 \tag{23}$$

where F_Z^1 and F_Z^2 = peak flood distributions for climatic regimes 1 and 2, respectively; and α^1 = probability of floods occurring in regime 1 in any given year. In some situations, such as ENSO in which frequent shifts may occur, the α^1 can be computed as the proportion of years in each regime. Although the lengths of the shifts in the flood observational records are not long enough to provide a reliable estimate of α^1 , the writers use a simple method to estimate the probability of a future extreme flood being in the first regime. Using the flood data for the period 1944–1997, and 1970 as the year of the shift from regime 1 to regime 2, α^1 was computed as 0.481. Alternatively, one could also use an AMO reconstructed from tree rings as in Enfield and Cid-Serrano (2006) as well as resampling to have a much longer data base to condition the proportion of years that floods occur in each regime. For example, the original AMO-reconstructed indices for a time span of 424 years showed nine periods of the AMO at the warm state and nine periods at the cool state with 217 and 189 years falling at those states, respectively (Enfield and Cid-Serrano 2006). Thus, this data will give $\alpha^1 = 0.53$ (instead of the 0.481 estimate based on the recorded flood-record length that exhibits only one shift). For the sake of illustration, the writers will continue the example using the value 0.481.

The writers fitted the GEV distribution using the location parameter as a function of the AMO regime and based on the likelihood ratio test it was determined that the Gumbel distribution was adequate for fitting the frequency distribution of annual floods of the St. Johns River. The location parameter of the Gumbel distribution has two values, 5,018 and 3,060 cfs, corresponding to the two AMO regimes [Fig. 12(a)]. The scale parameter is $\sigma = 2{,}094$ for both periods (using different scale parameters did not improve the model with respect to likelihood ratio). Whereas the flood-shifting regime that is related to the corresponding AMO shifting regime exhibits a local nonstationary behavior, in the long term it is assumed that the system is stationary, i.e., the shifting mechanism is stationary but with a mixed distribution. Therefore, the calculations

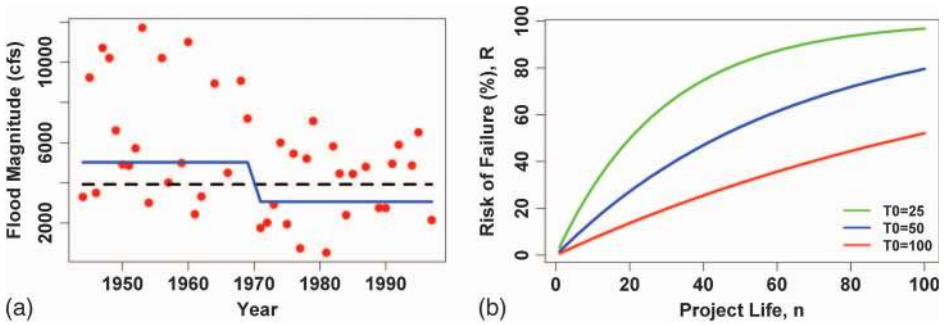

Fig. 12. (Color) (a) Peak floods of the St. Johns River at Christmas, Florida, and the location parameter estimated with a shift in flood regimes from AMO-warm to AMO-cold regimes; (b) risk of failure as a function of project life n

J. Hydrol. Eng. 2014.19:554-568.

of the return period and hydrologic risk as a function of project life n will be based on the corresponding equations for the stationary condition except that the underlying model is a mixed distribution [Fig. 12(b)].

The writers also compared the mixed model above versus a single Gumbel model (with 3,894 and 2,308 as the estimated location and scale parameters, respectively), and based on (1) the likelihood ratio test statistic ($D = 8.3$), (2) the chi-square at the 5% significance level (3.84), and (3) the p value 0.0039, the mixed Gumbel model was preferred over the single-Gumbel model. The writers compared the estimates of the return periods and risks one would obtain from the single-Gumbel model versus those for the mixed-Gumbel model using the value of $\alpha^1 = 0.481$. For example, the 100-year flood based on the single-Gumbel model becomes the 137-year flood for the mixed-Gumbel model. Likewise, the risks R obtained for a project life of 50 years are 39 and 31% for the single-Gumbel and mixed-Gumbel models, respectively. The diagnostic checks of the fitted mixed-Gumbel model gave acceptable results.

Further Remarks and Conclusion

Current practice of assuming stationarity in hydrologic extremes may not be applicable for some future engineering designs. The nonstationarity in extremes such as floods may be due to human influences in watersheds such as land-use changes, construction of dams, and changes in the climatic regime. Recent advances in addressing nonstationarity of extreme events have allowed the extension of the concepts of return period and risk into a nonstationary framework. Even though the writers' equations for determining the return period T and risk R that are applicable to nonstationary conditions were developed independently and without noticing and knowledge of previous work (as has occurred with many other papers published in the water literature as cited in other sections of this paper), the writers note previous developments by Olsen et al. (1998) in deriving T and R for nonstationary conditions, which are quite similar to those presented in this paper, but the essence of the derivations are different as explained in some detail in previous sections of this paper. The writers illustrated and applied the derived equations of T and R using several examples, including actual cases of increasing floods, increasing and decreasing sea-level extremes, and shifting flood-regimes arising from documented cases of human intervention in addition to climate variability and change. The applications demonstrated that the differences between the nonstationary return period and risk in addition to those corresponding to stationary conditions can be quite significant. They also suggest that a nonstationary analysis can be useful in making an appropriate assessment of the reliability (risk) of a hydraulic structure during the planned project-life. The methods and applications presented in this paper may be helpful to water resources specialists involved in planning and management of hydraulic structures at places impacted by anthropogenic effects and global climate change.

The derivations of T and R in this paper assume that the exceedance probability varies in accordance with time (consequently the parameters of the assumed GEV model also vary in accordance with time) and their computations (as illustrated in the examples and case studies) are based on the historical record. However, researchers must be cautious and recognize the limitations of the approach to use it with judgment for future applications. Under a nonstationary world a relevant question is what may be the realistic projections of the GEV model for the future? For example, consider the case for which it has been clearly shown that the cause of increasing floods in a particular basin is urbanization. If after several years of intense population growth and urbanization (and consequently increasing floods in accordance with time), urban dynamics studies indicate that such growth will decrease by half in the next 20 years and reach a built-out level (stabilized) in the following 20 years; the projected scenario is clear. A real example is the case of the Mercer River in Washington (Katz 2013), in which after intense growth (and increasing floods) for about 20 years the pattern of annual floods appears to have reached a constant mean level. However, in many cases such stabilizing pattern may not be apparent and estimating future projections may not be simple. Using synthetic time-series of peak discharges (Moglen 2003) and covariates of population density (e.g., Villarini et al. 2009b) may be useful. In general, there may be some uncertainty in such projections and researchers may consider alternative potential growth scenarios with estimates of their probability of occurrence. In addition, in case of increasing floods because of climate variability linked to a low frequency of oceanic and atmospheric processes, researchers may use covariates of climatic indices as in Sivapalan and Samuel (2009).

The nonstationary approach to return period and risk opens other opportunities that may be worth exploring. For example, it has been shown that the extension of the well-known geometric distribution to include time varying exceedance probabilities has allowed determining the return period and risk for nonstationary conditions of extreme events. In the case of stationary events, the well-known Binomial distribution enables researchers to determine the probability of y exceedances during the project life n of a hydraulic structure (for a project designed based on the return period $T = 1/p$.) It is also the basis for determining the reliability and risk of failure of a hydraulic structure. In this connection, the question that arises is whether it is possible to extend the binomial law so that it is applicable under a nonstationary framework. It would enable researchers to calculate the probability that, for example, three floods will exceed the design flood during the project life n given that the exceedance probabilities vary in accordance with time. In addition, the nonstationary applications reported in this paper have been based on the GEV distribution, which has been convenient because of the well-developed estimation procedures and easy features (such as expressing the cumulative distribution and quantile functions in explicit form, unlike other distributions such as those of the Pearson family). Thus, a natural extension would be applying the nonstationary concepts to other distributions for which the parameters may vary in accordance with time. The parameters of the nonstationary GEV distribution have been generally estimated based on the method of maximum likelihood but for the stationary GEV other methods (such as those based on the L-moments) may be more efficient, especially for small sample sizes. Therefore, possible extensions of estimation for nonstationary GEVs may use, for example, L-moments.

The writers' case studies discussed in this paper have been limited to maximum annual quantities such as annual extreme floods. However, the writers anticipate that more examples will arise from the research reported in this paper and a similar methodology will be applicable to a wide range of examples that include other processes and variables of interest in water resources (such as precipitation, wind, temperature, groundwater, and low flows). In addition, the methods could be extended considering larger data bases and the concepts of extreme order statistics (e.g., the m largest floods per year), peaks over thresholds (leading to a generalized Pareto family), Poisson point process, and even seasonality (e.g., thresholds varying periodically in accordance with time) as outlined in Coles (2001) and Katz (2010). Although the modeling

J. Hydrol. Eng. 2014.19:554-568.

process may become somewhat more involved it may lead to improving the estimates of flood-risk statistics.

Furthermore, based on the GEV family it is possible to determine the standard errors of parameters under nonstationary conditions. Coles (2001) and Cooley (2013) have suggested the delta method for determining the uncertainties of the T-year quantiles. However, this method requires the use of the approximate variance-covariance matrix of the nonstationary model parameters and the assumption of normality of the maximum likelihood estimators. Whereas this approach may provide practical estimates of the confidence intervals for the T-year extreme events for nonstationary models, further work may be needed to develop more rigorous approaches to consider the asymmetry that is generally associated with quantile estimators of extreme events. In addition, the inverse problem (i.e., determining the uncertainty of the nonstationary exceedance probabilities and how those uncertainties propagate to the uncertainty of the return period and risk) may be interesting topics to pursue.

Acknowledgments

The writers acknowledge P2C2, Multicentury Streamflow Records Derived from Watershed Modeling and Tree Ring Data, National Science Foundation (ATM-0823480). Furthermore, the writers thank Professors G. Villarini and R. M. Vogel for sharing their flood data in addition to their relevant comments and insights, and Dr. D. Cooley for his helpful suggestions. The writers acknowledge the University of Hawaii Sea Level Center for making available their hourly sea level data for the Key West and Adak tide gages. The writers also acknowledge the useful comments of the unknown reviewers and the efficient Editorial Board of the *Journal*.

References

Akintug, B., and Rasmussen, P. F. (2005). "A Markov switching model for annual hydrologic time series." *Water Resour. Res.*, 41(9), W09424.

Bindoff, N. L., et al. (2007). "Observations: Oceanic climate change and sea level." *Climate change 2007: The physical science basis*, Cambridge University Press, Cambridge, U.K.

Biondi, F., Kozubowski, T. J., Panorska, A. K., and Saito, L. (2008). "A new stochastic model of episode peak and duration for eco-hydro-climatic applications." *J. Ecol. Model.*, 211(3–4), 383–395.

Boes, D. C., and Salas, J. D. (1978). "Nonstationarity in the mean and the Hurst phenomenon." *Water Resour. Res.*, 14(1), 135–143.

Bras, R. L. (1990). *Hydrology: An introduction to hydrologic science*, Addison-Wesley, Reading, MA.

Caires, S., Swail, V. R., and Wang, X. L. (2006). "Projections and analysis of extreme wave climate." *J. Clim.*, 19(21), 5581–5605.

Chow, V. T., Maidment, D. R., and Mays, L. W. (1988). *Applied hydrology*, McGraw-Hill, New York.

Church, J. A., and White, N. J. (2011). "Sea-level rise from the late 19th to the early 21st century." *Surv. Geophys.*, 32(4–5), 585–602.

Cohn, T., and Lins, H. F. (2005). "Nature's style: Naturally trendy." *Geophys. Res. Lett.*, 32(23), L23402.

Coles, S. (2001). *An introduction to statistical modeling of extreme values*, Springer, London.

Cooley, D. (2009). "Extreme value analysis and the study of climate change." *Clim. Change*, 97(1–2), 77–83.

Cooley, D. (2013). "Return periods and return levels under climate change." Chapter 4, *Extremes in a changing climate: Detection, analysis and uncertainty*, A. AghaKouchak, D. Easterling, and K. Hsu, eds., Vol. 65, Springer, New York.

Douglas, E. M., Vogel, R. M., and Kroll, C. N. (2000). "Trends in floods and low flows in the United States: Impact of spatial correlation." *J. Hydrol.*, 240(1–2), 90–105.

El Adlouni, A., Ouarda, T. B. M., Zhang, X., Roy, R., and Bobee, B. (2007). "Generalized maximum likelihood estimators for the nonstationary generalized extreme value model." *Water Resour. Res.*, 43(3), W03410.

Enfield, D. B., and Cid-Serrano, L. (2006). "Projecting the risk of future climate shifts." *Int. J. Clim.*, 26(7), 885–895.

Enfield, D. B., Mestas-Nunez, A. M., and Trimble, P. J. (2001). "The Atlantic Multidecadal Oscillation and its relation to rainfall and river flows in the continental U.S." *Geophys. Res. Lett.*, 28(10), 2077–2080.

extREMES [Computer software]. Unive. Corporation for Atmospheric Research (UCAR), National Center for Atmospheric Research (NCAR), Boulder, CO.

Fortin, V., Perreault, L., and Salas, J. D. (2004). "Retrospective analysis and forecasting of streamflows using a shifting level model." *J. Hydrol.*, 163–135 ,(1)296.

Frances, F., Salas, J. D., and Boes, D. C. (1994). "Flood frequency analysis with systematic and historical or paleoflood data based on two-parameter general extreme value models." *Water Resour. Res.*, 30(6), 1653–1664.

Franks, S. W., and Kuczera, G. (2002). "Flood frequency analysis: Evidence and implications of secular climate variability, New South Wales." *Water Resour. Res.*, 38(5), 20-1–20-7.

Gash, J. H. C., and Nobre, C. A. (1997). "Climatic effects of Amazonian deforestation: Some results from ABRACOS." *Bull. Am. Meteorol. Soc.*, 78(5), 823–830.

Gilroy, K. L., and McCuen, R. H. (2012). "A nonstationary flood frequency analysis method to adjust for future climate change and urbanization." *J. Hydrol.*, 414–415(1), 40–48.

Griffis, V., and Stedinger, J. R. (2007). "Incorporating climate change and variability into bulletin 17B LP3 model." *Proc., World Environmental and Water Resources Congress*, ASCE, Reston, VA, 1–8.

Guilleland, E., and Katz, R. W. (2011). "New software to analyze how extremes change over time." *EOS Trans. Am. Geophys. Union*, 92(2), 13–14.

Gumbel, E. J. (1941). "The return period of flood flows." *Ann. Math. Stat.*, 12(2), 163–190.

Hejazi, M. I., and Markus, M. (2009). "Impacts of urbanization and climate variability on floods in northeastern Illinois." *J. Hydrol. Eng.*, 10.1061/(ASCE)HE.1943-5584.0000020, 606–616.

Hirsch, R. M., and Ryberg, K. R. (2012). "Has the magnitude of floods across the USA changed with global CO2 levels?" *Hydr. Sci. J.*, 57(1), 1–9.

Houston, J. R. (2012). "Global sea level projections to 2100 using methodology of the Intergovernmental Panel on Climate Change." *J. Waterway, Port, Coastal, Ocean Eng.*, 10.1061/(ASCE)WW.1943-5460.0000158, 82–87.

Houston, J. R., and Dean, R. G. (2011). "Sea-level acceleration based on U.S. tide gauges and extensions of previous global-gauge analyses." *J. Coastal Res.*, 27(3), 409–417.

Interagency Committee on Water Data (IACWD). (1982). "Guidelines for determining flood flow frequency." *Bulletin 17B*, Office of Water Data Coordination, USGS, Reston, VA.

Int. Panel on Climate Change (IPCC). (2007). *Climate change 2007: The physical science basis. Contribution of working group I to the fourth assessment report of the Intergovernmental Panel on Climate Change*, S. Solomon, et al., eds., Cambridge University Press, Cambridge, U.K.

Jain, S., and Lall, U. (2000). "Magnitude and timing of annual maximum floods: Trends and large-scale climatic associations for the Blacksmith Fork River, Utah." *Water Resour. Res.*, 36(12), 3641–3651.

Jain, S., and Lall, U. (2001). "Floods in a changing climate: Does the past represent the future?" *Water Resour. Res.*, 37(12), 3193–3205.

Katz, R. W. (1993). "Towards a statistical paradigm for climate change." *Clim. Res.*, 2(1), 167–175.

Katz, R. W. (2010). "Statistics of extremes in climate change." *Clim. Change*, 100(1), 71–76.

Katz, R. W. (2013). "Statistical methods for nonstationary extremes." Chapter 2, *Extremes in a changing climate: Detection, analysis and uncertainty*, A. AghaKouchak, D. Easterling, and K. Hsu, eds., Vol. 65, Springer, New York.

Katz, R. W., Parlange, M. B., and Naveau, P. (2002). "Statistics of extremes in hydrology." *Adv. Water Resour.*, 25(8), 1287–1304.

Kiem, A. S., Franks, S. W., and Kuczera, G. (2003). "Multi-decadal variability of flood risk." *Geophys. Res. Lett.*, 30(2), GL015992.

Knutson, T. R., et al. (2010). "Tropical cyclones and climate change." *Nat. Geosci.*, 3(3), 157–163.

Konrad, C. P., and Booth, D. B. (2002). "Hydrologic trends associated with urban development for selected streams in the Puget Sound Basin, western Washington." *USGS Water Resources Investigations Rep. 02-4040*, United States Geological Survey, Tacoma, WA.

Kunkel, K. E., Easterling, D. R., Kristovich, A. R., Gleason, B., Stoecker, L., and Smith, R. (2010). "Recent increases in US heavy precipitation associated with tropical cyclones." *Geophys. Res. Lett.*, 37(24), L24706.

Leadbetter, M. R. (1983). "Extremes and local dependence in stationary sequences." *Probab. Theory Related Fields*, 65(2), 291–306.

Lins, H. F., and Slack, J. R. (1999). "Streamflow trends in the United States." *Geophys. Res. Lett.*, 26(2), 227–230.

Mandelbaum, M., Hlynka, M., and Brill, P. H. (2007). "Nonhomogeneous geometric distributions with relations to birth and death processes." *Sociedad de estadistica e investigacion operativa*, Springer, New York, 281–296.

Mantua, N. J., Hare, S. R., Zhang, Y., Wallace, J. M., and Francis, R. C. (1997). "A Pacific Interdecadal Climate Oscillation with impacts on salmon production." *Bull. Am. Meteorol. Soc.*, 78(6), 1069–1079.

McCabe, G. J., and Wolock, D. M. (2002). "A step increase in streamflow in the conterminous United States." *Geophys. Res. Lett.*, 29(24), GL015999.

Menendez, M., and Woodworth, P. L. (2010). "Changes in extreme high water levels based on a quasi-global tide-gauge data set." *J. Geophys. Res. Oceans*, 115(C10), JC005997.

Milly, P. C. D., et al. (2008). "Stationarity is dead: Whither water management?" *Science*, 319(5863), 573–574.

Moglen, G. E. (2003). "Frequency analysis under nonstationary land use conditions." Chapter 13, *Modeling hydrologic change–Statistical methods*, R. H. McCuen, ed., Lewis Publishers, Boca Raton, FL.

Mood, A., Graybill, F., and Boes, D. C. (1974). *Introduction to the theory of statistics*, 3rd Ed., McGraw-Hill, New York.

National Research Council (NRC). (1987). *Responding to changes in sea level: Engineering implications*, National Academies, Washington, DC.

Ng, M., and Vogel, R. M. (2010). "Multivariate non-stationary stochastic streamflow models for two urban watersheds." *Proc., Environmental and Water Resources Institute World Congress*, ASCE, Reston, VA, 2550–2561.

Obeysekera, J., Irizarry, M., Park, J., Barnes, J., and Dessalegne, T. (2011). "Climate change and its implications for water resources management in south Florida." *Stoch. Environ. Res. Risk Assess.*, 25(4), 495–516.

Obeysekera, J., and Park, J. (2013). "Scenario-based projections of extreme sea levels." *J. Coast Res.*, 29(1), 1–7.

Obeysekera, J., Park, J., Irizarry-Ortiz, M., Barnes, J., and Trimble, P. (2012). "Probabilistic projection of mean sea level and coastal extremes." *J. Waterway, Port, Coastal, Ocean Eng.*, 10.1061/(ASCE)WW.1943-5460.0000154, 135–141.

Olsen, J. R., Lambert, J. H., and Haimes, Y. Y. (1998). "Risk of extreme events under nonstationary conditions." *Risk Anal.*, 18(4), 497–510.

Olsen, J. R., Stedinger, J. R., Matalas, N. C., and Stakhiv, E. Z. (1999). "Climate variability and flood frequency estimation for the Upper Mississippi and Lower Missouri rivers." *J. Am. Water Resour. Assoc.*, 35(6), 1509–1523.

Parey, S., Malek, F., Laurent, C., and Dacunha-Castelle, D. (2007). "Trends and climate evolution: Statistical approach for very high temperatures in France." *Clim. Change*, 81(3), 331–352.

Park, J., Obeysekera, J., Barnes, J., Irizarry, M., and Park-Said, W. (2010). "Climate links and variability of extreme sea level events at Key West, Pensacola, and Mayport Florida." *J. Waterway, Port, Coastal, Ocean Eng.*, 10.1061/(ASCE)WW.1943-5460.0000052, 350–356.

Park, J., Obeysekera, J., Irizarry, M., Barnes, J., Trimble, P., and Park-Said, W. (2011). "Storm surge projections and implications for water management in south Florida." *Clim. Change*, 107(1–2), 109–128.

Pielke, R. A., Sr., et al. (2007). "An overview of regional land-use and land-cover impacts on rainfall." *Tellus B*, 59(3), 587–601.

Potter, K. W. (1976). "Evidence for nonstationarity as a physical explanation of the Hurst phenomenon." *Water Resour. Res.*, 12(5), 1047–1052.

Rahmstorf, S. (2007). "A semi-empirical approach to projecting future sea-level rise." *Science*, 315(5810), 368–370.

Rao, D. V. (2009). "Discussion of 'Log-Pearson type 3 distribution and its application in flood frequency analysis. II: Parameter estimation methods' by V. W. Griffis and J. R. Stedinger." *J. Hydrol. Eng.*, 10.1061/(ASCE)1084-0699(2009)14:2(207), 492–500.

Rossi, F., Fiorentino, M., and Versace, P. (1984). "Two-component extreme value distribution for flood frequency analysis." *Water Resour. Res.*, 20(7), 847–856.

Ruggiero, P., Komar, P. D., and Allan, J. C. (2010). "Increasing wave heights and extreme value projections of the wave climate of the U.S. Pacific Northwest." *Coastal Eng.*, 57(5), 539–552.

Salas, J. D., and Boes, D. C. (1980). "Shifting level modeling of hydrologic series." *Adv. Water Resour.*, 3(2), 59–63.

Sallenger, A. H., Doran, K. S., and Howd, P. A. (2012). "Hotspot of accelerated sea-level rise on the Atlantic coast of North America." *Nat. Clim. Change*, 2(12), 884–888.

Schilling, K. E., and Libra, R. D. (2003). "Increased baseflow in Iowa over the second half of the 20th century." *J. Am. Water Resour. Assoc.*, 39(4), 851–860.

Sivapalan, M., and Samuel, J. M. (2009). "Transcending limitations of stationarity and the return period: Process-based approach to flood estimation and risk assessment." *Hydrol. Process.*, 23(11), 1671–1675.

Stedinger, J. R., and Cohn, T. A. (1986). "Flood frequency analysis with historical and paleoflood information." *Water Resour. Res.*, 22(5), 785–793.

Strupczewski, W. G., Singh, V. P., and Mitosek, H. T. (2001). "Non-stationary approach to at-site flood frequency modeling. III. Flood frequency analysis of Polish rivers." *J. Hydrol.*, 248(1), 152–167.

Sveinsson, O. G. B., Salas, J. D., and Boes, D. C. (2005). "Prediction of extreme events in hydrologic processes that exhibit abrupt shifting patterns." *J. Hydrol. Eng.*, 10.1061/(ASCE)1084-0699(2005)10:4(315), 315–326.

Sveinsson, O. G. B., Salas, J. D., Boes, D. C., and Pielke, R. A. (2003). "Modeling the dynamics of long-term variability of hydroclimatic processes." *J. Hydrometeor.*, 4(3), 489–505.

Trimble, P., Obeysekera, J., Cadavid, L., and Santee, E. R. (2006). "Applications of climate outlooks for water management in south Florida." *Climate variations, climate change, and water resources engineering*, J. D. Garbrecht and T. C. Piechota, eds., ASCE, Reston, VA.

U.S. Army Corps of Engineers (USACE). (2011). "Sea-level change considerations in civil works programs." *Engineering Circular No. 1165-2-212-1*, Dept. of the Army, Washington, DC.

Vermeer, M., and Rahmstorf, S. (2009). "Global sea level linked to global temperature." *Proc. Natl. Acad. Sci.*, 106(51), 21527–21532.

Viessman, W., Jr., and Lewis, G. L. (2003). *Introduction to hydrology*, 5th Ed., Addison-Wesley, Reading, MA.

Villarini, G., Smith, J. A., and Napolitano, F. (2010). "Nonstationary modeling of a long record of rainfall and temperature over Rome." *Adv. Water Resour.* 33(10), 1256–1267.

Villarini, G., Serinaldi, F., Smith, J. A., and Krajewski, W. F. (2009a). "On the stationarity of annual flood peaks in the continental United States during the 20th century." *Water Resour. Res.*, 45(8), W08417.

Villarini, G., Smith, J. A., Serinaldi, F., Bales, J., Bates, P. D., and Krajewski, W. F. (2009b). "Flood frequency analysis for nonstationary annual peak records in an urban drainage basin." *Adv. Water Resour.*, 32(8), 1255–1266.

Vogel, R. M., Yaindl, C., and Walter, M. (2011). "Nonstationarity: Flood magnification and recurrence reduction factors in the United States." *J. Am. Water Resour. Assoc.*, 47(3), 464–474.

Walter, M., and Vogel, R. M. (2010). "Increasing trends in peak flows in the northeastern United States and their impacts on design." *Proc., Joint Federal Interagency Conf.*, Advisory Committee on Water Information, USGS, Reston, VA, 1–16.

Watson, P. J. (2011). "Is there evidence yet of acceleration in mean sea level rise around mainland Australia?" *J. Coastal Res.*, 27(2), 368–377.

Waylen, P. R., and Caviedes, C. N. (1986). "El Niño and annual floods on the Peruvian litoral." *J. Hydrol.*, 89(1–2), 141–156.

Wigley, T. M. L. (2009). "The effect of changing climate on the frequency of absolute extreme events." *Climatic Change*, 97(1–2), 67–76.

Wigley, T. M. L. (1988). "The effect of climate change on the frequency of absolute extreme events." *Clim. Monit.*, 17(1–2), 44–55.